

# Study of Ionospheric Delay Gradient Based on GPS Monitoring Stations Near Suvarnabhumi Airport in Thailand

Sarawoot Rungraengwajiake, Pornchai Supnithi, Susumu Saito, Nattapong Siansawasdi, and Apitep Saekow

**Abstract** The ionospheric delay gradient is an important parameter for the planning of ground-based augmentation system (GBAS) in a region. When it is beyond the limit, the integrity and safety for landing approach of CAT II/III may be compromised. In order to maintain the availability and safety requirement of the system, the ionospheric threat models have been developed in several countries during the past few years. However, the ionospheric delay gradient associated with plasma bubble in low latitude region has not been studied well. In this work, we present some analytical results of ionospheric delay gradient based on three GPS monitoring stations near Suvarnabhumi airport in Thailand. The stations are located on the campus of King Mongkut's Institute of Technology Ladkrabang (13.7278°N, 100.7726°E), Stamford University (13.7356°N, 100.6612°E) and Suvarnabhumi airport (13.6945°N, 100.7608°E). The analyzed results on 1st September 2011 show that the ionospheric delay gradient varies from  $-95.23$  to  $107.7$  mm/km during the occurrence of the plasma bubbles.

**Keywords** GBAS • Ionospheric delay gradient • Slant TEC

---

S. Rungraengwajiake (✉) • P. Supnithi  
Faculty of Engineering, King Mongkut's Institute of Technology Ladkrabang,  
Bangkok 10520, Thailand  
e-mail: [sarawootersky@gmail.com](mailto:sarawootersky@gmail.com)

S. Saito  
Communication, Navigation and Surveillance Department,  
Electronic Navigation Research Institute, Tokyo, Japan

N. Siansawasdi  
Air Navigation Radio Aids Department, Aeronautical Radio of Thailand, Bangkok, Thailand

A. Saekow  
Faculty of Science and Technology, Stamford International University, Bangkok, Thailand

## 1 Introduction

The global navigation satellite system (GNSS) has become a powerful component for aeronautical navigations. However, the ionospheric delay is still the largest source of errors and degrades the accuracy of GNSS receivers. To improve the accuracy and availability of the system, the differential techniques have been developed to mitigate such error. For aeronautical navigation, the Satellite-Based Augmentation System (SBAS) and Ground-Based Augmentation System (GBAS) have been developed to support all navigation operational levels of the aircrafts. These augmentation systems provide the differential corrections and integrity information to the GNSS receivers that are equipped in the aircrafts. It is now well known that the severe ionospheric disturbances such as the storm-enhanced density (SED) can cause a large ionospheric delay gradient, which affects the availability and integrity requirement of the systems especially for landing approach of GBAS CAT II/III. The previous study in [1] has shown the extreme ionospheric delay gradient observed in U.S. on 20th November 2003 during the geomagnetic storm. It can reach 413 mm/km over the 40–100 km baselines. Therefore, the ionospheric anomaly monitoring and ionospheric threat model for GBAS are developed based on GPS receivers of CONUS (Conterminous U.S.), emphasizing on this extreme event located only in U.S. [2]. In order to protect the safety level requirements for worldwide operation, however, the local ionospheric threat model needs to be developed for other concerned regions. For equatorial and low-latitude regions, particularly, the equatorial anomaly and plasma bubble are common phenomena which can cause the ionospheric delay gradient as well as ionospheric scintillation [3]. However, the ionospheric delay gradients associated with plasma bubble in these regions have not been well studied [4].

In this work, we investigate the ionospheric delay gradient obtained from GPS monitoring stations near Suvarnabhumi airport in Bangkok, Thailand. We have analyzed a sample set of data during September equinox with the plasma bubble occurrence. In addition, we show a simple concept to calibrate the receiver biases suitable for the satellite pass during plasma bubble occurrence.

## 2 Theoretical Background

The largest error source of GNSS such as Global Positioning System (GPS) measurements is the ionospheric delay ( $I$ ), which is a proportional to the amount of electrons in terms of slant total electron content (STEC), i.e.,

$$I = \frac{40.3}{f^2} STEC \quad (1)$$

where  $f$  is the frequency of the satellite signal and  $STEC$  is a number of electrons found in  $1\text{-m}^2$  column along the satellite-receiver propagation path, generally expressed in TEC unit or TECU ( $1 \text{ TECU} = 10^{16} \text{ electron/m}^2$ ). For GPS system, the slant TEC can be derived from dual-frequency GPS receivers based on the combination of pseudorange ( $STEC_P$ ) or carrier phase ( $STEC_L$ ) measurements given by

$$STEC_P = K(P_2 - P_1) \quad (2)$$

and

$$STEC_L = K(L_1 - L_2) \quad (3)$$

where  $P_1$ ,  $P_2$ ,  $L_1$  and  $L_2$  are the pseudorange and carrier phase (expressed in range) measurements at the L1 (1575.42 MHz) and L2 frequency (1227.60 MHz), respectively. The constant  $K = 9.5196 \text{ m}^{-1} \text{ TECU}$  for  $STEC$  expressed in TECU ( $1 \text{ TECU} = 10^{16} \text{ electrons/m}^2$ ). For the L1 and L2 frequency, 1 TECU is equivalent to 16 and 27-cm time delay. Note that the  $STEC_P$  still includes the inherent satellite and receiver inter-frequency bias (IFB) which comes from the differential extra delay time between L1 and L2 frequencies due to the internal electronic circuit of receiver front-end and also some from satellite antenna path. Although the slant TEC derived from the pseudorange measurements is noisier than that derived from the carrier phase measurements, the carrier phase measurement contains initial phase ambiguities, which frequently cause the slant TEC to have some negative values. In order to keep the precise slant TEC from carrier phase measurement and also remove the initial phase ambiguities, the  $STEC_L$  is adjusted to the  $STEC_P$  level. For a simple approach, the  $STEC_L$  is adjusted to the mean value of corresponding  $STEC_P$  for each continuous arc, which can be expressed as

$$STEC_{adj} = STEC_L + (\overline{STEC_P - STEC_L})_{arc} \quad (4)$$

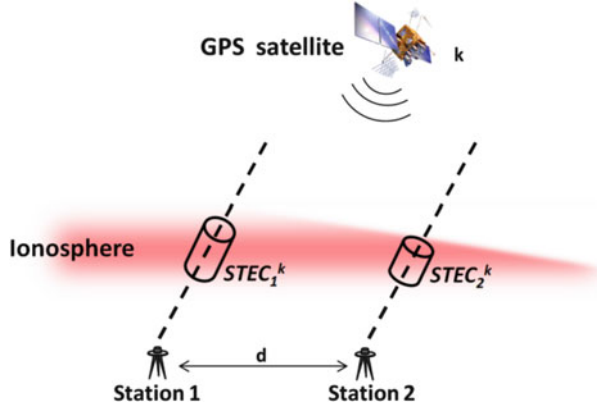
where  $\bar{x}$  represents the mean of  $x$ . However, the satellite and receiver IFB still needs to be accounted for. The adjusted slant TEC ( $STEC_{adj}$ ) can therefore be given by

$$STEC_{adj} = STEC + B_S + B_R \quad (5)$$

where  $B_S$  and  $B_R$  are the satellite and receiver IFB, respectively. To compute the ionospheric delay gradient, the differential  $STEC_{adj}$  of the  $k$ th satellite between two monitoring stations is first computed. Therefore, the satellite IFB will be eliminated. Figure 1 shows the concept of ionospheric delay gradient computation. However, the differential receiver IFB ( $B_{R1} - B_{R2}$ ) still remains as a significant offset, i.e.,

$$dSTEC^k = (STEC_1^k - STEC_2^k) + (B_{R1} - B_{R2}) \quad (6)$$

**Fig. 1** Illustration of ionospheric delay gradient monitoring stations



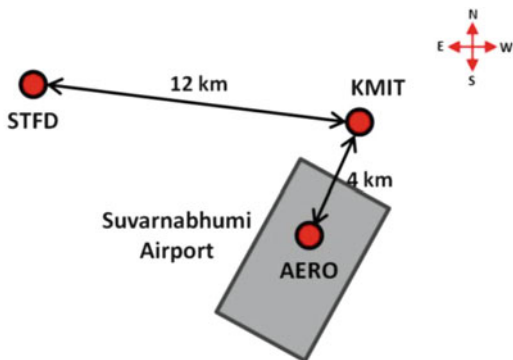
The next step is to remove the differential receiver IFB ( $B_{R1} - B_{R2}$ ). We apply the principle that the slant TECs of a short baseline monitoring stations are similar during the quiet ionospheric condition. Also, we assume that the receiver IFBs do not vary in one day. Therefore, the constant of the differential  $STEC_{adj}$  is just the differential receiver IFB ( $B_{R1} - B_{R2}$ ). This method is simpler than the methods in [5, 6]. Finally, the ionospheric delay gradient ( $\nabla I$ ) can be estimated by dividing the differential  $STEC_{adj}$  between two stations by the baseline distance ( $d$ ) between two receivers at each epoch  $t$ , i.e.,

$$\nabla I(t) = \frac{40.3}{f^2} \left( \frac{STEC_1^k(t) - STEC_2^k(t)}{d} \right) \quad (7)$$

### 3 Experimental Setup

The slant TECs are derived from RINEX (Receiver Independent Exchange Format) data of three dual-frequency GPS receivers at the monitoring stations near Suvarnabhumi airport in Bangkok, Thailand. One is located on the runway of the airport (AERO: 13.6945°N, 100.7608°E). The others are located at King Mongkut's Institute of Technology Ladkrabang (KMIT: 13.7278°N, 100.7726°E) and Stamford International University (STFD: 13.7356°N, 100.6612°E) which are shown in Fig. 2. The pseudorange and carrier phase measurements are made at a 1-Hz sampling interval. In the pre-processing step, the cycle slips in the carrier phase measurements are detected and repaired using the algorithm in [7]. In this work, we select the data on 1st September 2011 for the analysis, which has the solar 10.7 cm radio flux index (F10.7) equal to 112, and we found the  $STEC$  fluctuations during nighttime.

**Fig. 2** Three GPS monitoring stations near Suvarnabhumi airport



### 4 Results and Discussions

In Fig. 3, we show the *STEC* of three stations on 1st September 2011. Note that the satellite and receiver IFBs are not calibrated and there are no *STEC* data from AERO station during 00:00–05:00 UT due to the receiver problems. The *STEC* of all stations evidently fluctuate during 14:00–19:00 UT or 21:00–02:00 LT (UTC + 7). The *STEC* fluctuation observed at low-latitude regions during nighttime are possibly caused by plasma bubbles. There are five satellites (PRN2, PRN9, PRN14, PRN21 and PRN29), which are affected by the *STEC* disturbances during this time.

In Fig. 4, we show the differential *STEC* (*dSTEC*) of these satellites aligning in the STFD-KMIT and AERO-KMIT directions or west–east and south–north direction, which can be considered zonal and meridional baselines, respectively. The different colors indicate the *dSTEC* of the visible satellites. The *dSTEC*s also evidently start the fluctuation during 14:00–19:00 UT in both directions. The *dSTEC*s in the STFD-KMIT baseline has higher fluctuation than the AERO-KMIT baseline, probably caused by the longer baseline and the zonal drift of plasma bubble. The *dSTEC* values are relatively constant during 09:00–13:00 and 19:00–24:00 UT. This constant level can be regarded as the differential receiver IFBs. The average of the constant level of *dSTEC*s is considered the differential receiver IFBs which is then subtracted from the original *dSTEC*s. However, a slight offset exists in the AERO-KMIT direction due to the uncertainty in the adjustment process as detailed in [8]. The differential receiver IFBs should therefore be considered for each satellite. The differential receiver IFBs can vary from 4.28 to 5.12 TECU for STFD-KMIT receiver and 5.18 to 6.78 TECU for AERO-KMIT receiver. After the bias calibration, the ionospheric delay gradient ( $\nabla I$ ) with respect to the L1 frequency is shown in Fig. 5.

The  $\nabla I$  trends of both directions look similar with the fluctuation starting around 13:30 UT and becoming flat at 20:00 UT. The maximum  $\nabla I$  can reach 107.7 mm/km at AERO-KMIT direction observed from PRN29 around 14:30 UT. For STFD-KMIT direction, the PRN21 gives the maximum  $\nabla I = -95.23$  mm/km at 16:00 UT. In addition, the  $\nabla I$  fluctuation of some satellites (for example, PRN9 (green)

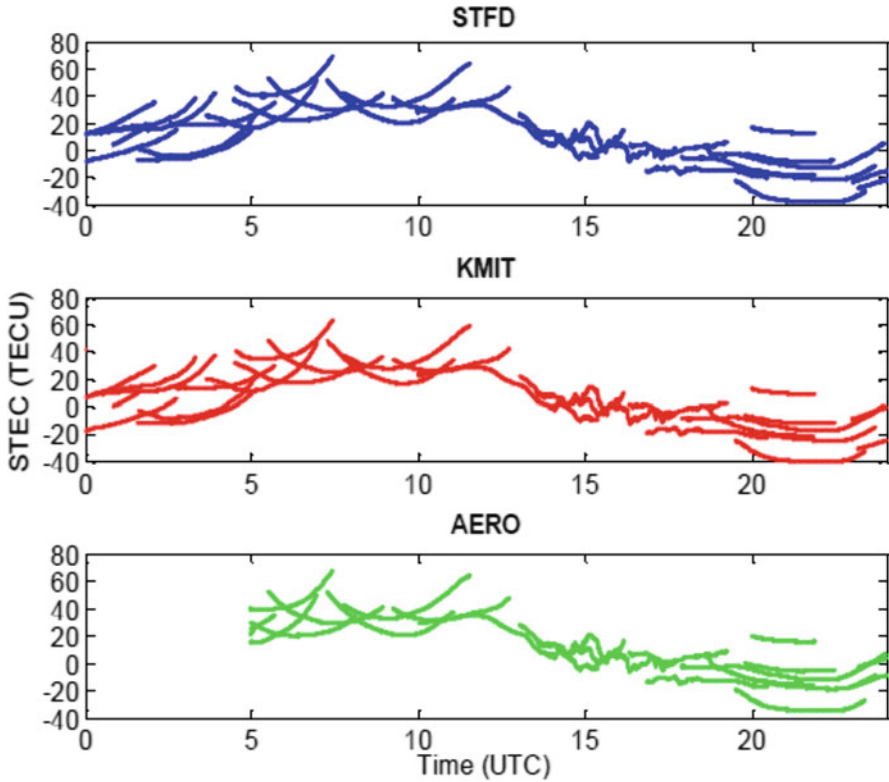


**Fig. 3** Overall slant TECs of three stations (satellite and receiver IFBs are not calibrated)

and PRN14 (pink)) evidently show the different patterns. This can be due to the combination effect of IPP (Ionospheric Pierce Point) motions and plasma bubble movement. In order to evaluate the effects of plasma bubble on GBAS, the current plasma bubble model applies a rectangular depletion shape of electron density to simulate the worst case of positioning error [4]. However, the  $\nabla I$  results show that they have the complicated variation corresponding to the complex shapes of plasma bubble. Figure 6 shows the probability mass functions (PMFs) of the ionospheric delay gradient ( $\nabla I$ ) of both directions. The average and standard deviation of  $\nabla I$  in STFD-KMIT and AERO-KMIT directions are 1.16 and  $-1.36$  mm/km, 12.52 and 7.81 mm/km, respectively. The distribution centers of both directions are close to zero. The deviation of both directions look symmetrical with the STFD-KMIT direction showing more deviation than AERO-KMIT direction, probably caused by the moving of plasma bubble in the zonal direction. In order to support all possibilities of ionospheric delay gradient on this day, the local ionospheric threat model should cover the lower and upper bound of these PMFs, which are  $-95.23$  to 107.7 mm/km. For the GAST-D (GBAS Approach Service Type D), which is the single-frequency GBAS support for CAT II/III, the current SARPs (Standards

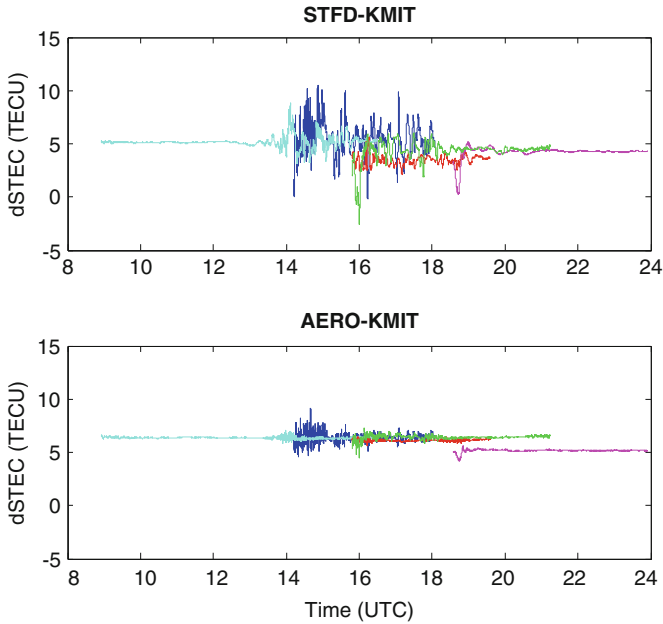


**Fig. 4** Differential *STEC* (*dSTEC*) align in STFD-KMIT (*top*) and AERO-KMIT (*bottom*) direction

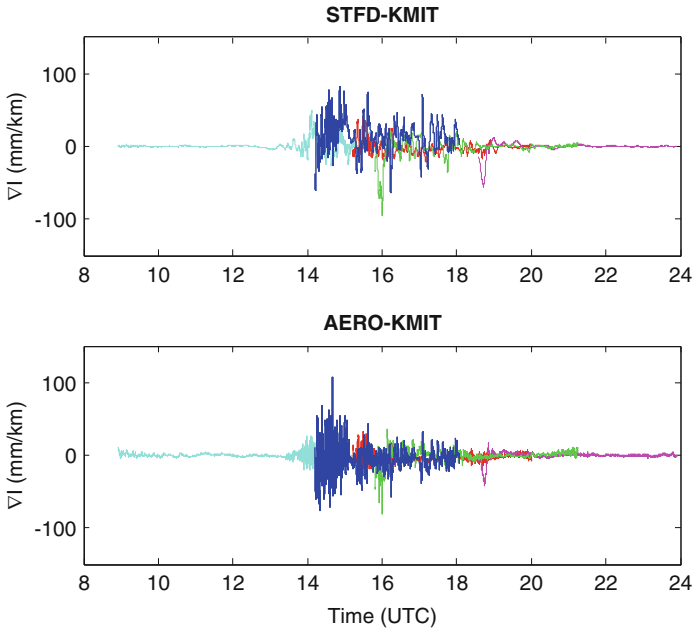


**Fig. 5** Ionospheric delay gradient ( $\nabla I$ ) align in STFD-KMIT (*top*) and AERO-KMIT (*bottom*) direction

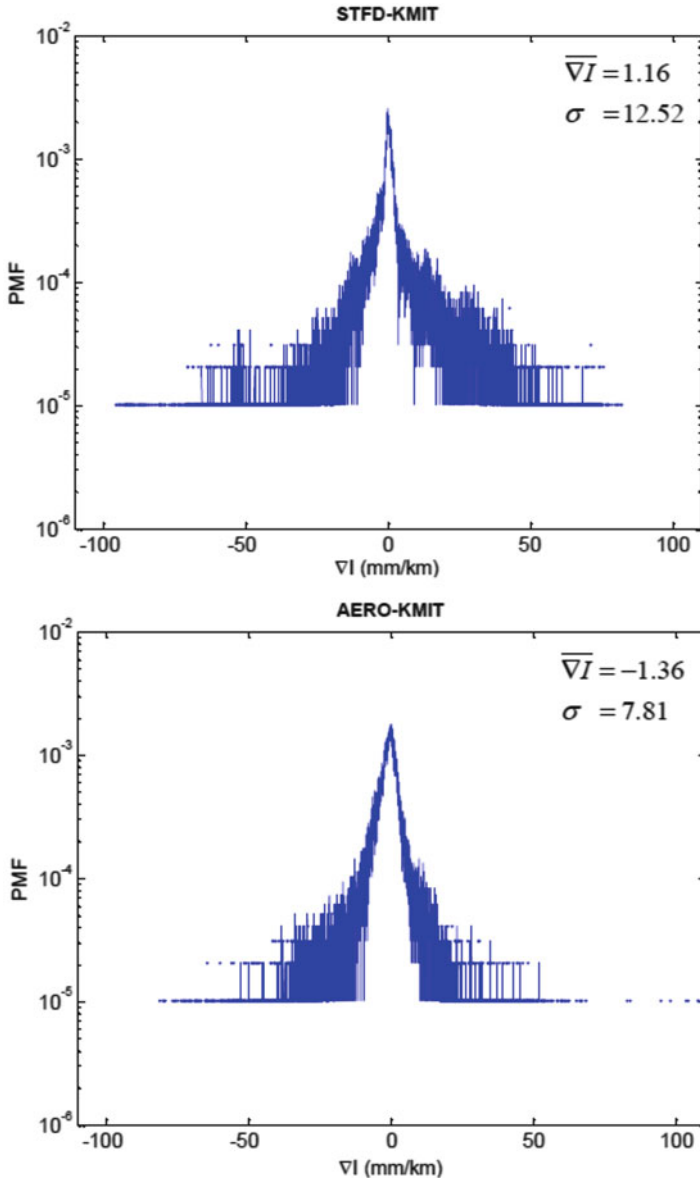


**Fig. 6** Probability mass functions (PMFs) of ionospheric delay gradient ( $\nabla I$ ) in STFD-KMIT (*top*) and AERO-KMIT (*bottom*) direction



and Recommended Practices) requires the ionospheric delay gradient shall be less than 300 mm/km [9]. Although, the observed ionospheric delay gradients during plasma bubble occurrence in this study are lower than the requirement threshold, the monitoring stations should continue to investigate more data sets to identify the possible extreme events within this region.

## 5 Conclusion

The ionospheric delay gradient is an important parameter for integrity and availability monitoring of GBAS. The equatorial and low-latitude regions are well known to have the plasma bubble phenomenon which may potentially degrade the GBAS system performance. In this work, we have analyzed the ionospheric delay gradient from three monitoring stations near Suvarnabhumi airport in Bangkok, Thailand. The results show the ionospheric delay gradient at the west–east and south–north directions can vary from  $-95.23$  to  $107.7$  mm/km on the studied day in September equinox.

**Acknowledgments** The authors are grateful to Aeronautical Radio of Thailand, KMITL and Stamford International University for providing the location and facilities for the GPS receiver installation. This work is partially funded by National Research Council of Thailand and KMITL Research Fund.

## References

1. Datta-Barua S, Lee J, Pullen S, Luo M, Ene A, Qiu D, Zhang G, Enge P (2010) Ionospheric threat parameterization for local area GPS-based aircraft landing systems. *J Aircr* 47:1141–1151
2. Lee J, Jung S, Bang E, Pullen S, Enge P (2010) Long term monitoring of ionospheric anomalies to support the local area augmentation system. In: *Proceeding of ION GNSS 2010*, pp 2651–2660
3. Yoshihara T, Fujii N, Matsunaga K, Hoshino K, Sakai T, Wakabayashi S (2007) Preliminary analysis of ionospheric delay variation effect on GBAS due to plasma bubble at southern region in Japan. In: *Proceeding of the 2007 National Technical Meeting of ION 2007*, pp 1065–1072
4. Saito S, Yoshihara T, Fujii N (2009) Study of effects of the plasma bubble on GBAS by a three-dimensional ionospheric delay model. In: *Proceeding of ION GNSS 2009*, pp 1141–1148
5. Ma G, Maruyama T (2003) Derivation of TEC and estimation of instrumental biases from GEONET in Japan. *Ann Geophys* 21:2083–2093
6. Rideout W, Coster A (2006) Automated GPS processing for global total electron content. *GPS Solutions* 10:219–228
7. Blewitt G (1990) An automatic editing algorithm for GPS data. *Geophys Res Lett* 17:199–202
8. Ciruolo L, Azpilicueta E, Brunini C, Meza A, Radicella SM (2007) Calibration errors on experimental slant total electron content (TEC) determined with GPS. *J Geod* 81:111–120
9. Murphy T, Harris M, Pullen S, Pervan B, Saito S, Brenner M (2010) Validation of ionospheric anomaly mitigation for GAST-D. In: *ICAO NSP Working Group of the Whole (WGW) meeting, Montreal*